Organic & Biomolecular Chemistry

Cite this: *Org. Biomol. Chem.*, 2011, **9**, 1948

www.rsc.org/obc

PAPER

Dendri-RAFTs: a second generation of cyclopeptide-based glycoclusters†

Isabelle Bossu,[a] Miroslav Šulc,[b] Karel Křenek,[b] Emilie Dufour,[a] Julian Garcia,[a] Nathalie Berthet,[a] Pascal Dumy,[a] Vladimír Křen*[b] and Olivier Renaudet*[a]

Received 23rd September 2010, Accepted 15th November 2010
DOI: 10.1039/c0ob00772b

Synthetic glycoclusters and their related biological applications have stimulated increasing interest over the last decade. As a prerequisite to discovering active and selective therapeuticals, the development of multivalent glycoconjugates with diverse topologies is faced with inherent synthetic and structural characterisation difficulties. Here we describe a new series of molecularly-defined glycoclusters that were synthesized in a controlled manner using a robust and versatile divergent protocol. Starting from a Regioselectively Addressable Functionalized Template (RAFT) carrier, either a polylysine dendritic framework or a second RAFT, then 16 copies of βGal, αMan, βLac or cancer-related Thomsen-Freidenreich (αTF) antigen were successively conjugated within the same molecule using oxime chemistry. We thus obtained a new generation of dendri-RAFTs glycoclusters with high glycosidic density and variable spatial organizations. These compounds displaying 16 endgroups were unambiguously characterized by NMR spectroscopy and mass spectrometry. Further biological assays between a model lectin from *Canavalia ensiformis* (ConA) and mannosylated glycoclusters revealed a higher inhibition potency than the tetravalent counterpart, in particular for the hexadecavalent polylysine skeleton. Together with the efficiency of the synthetic and characterisation processes, this preliminary biological study provided clear evidence of promising properties that make the second generation of cyclopeptide-based glycoclusters attractive for biomedical applications.

Introduction

Understanding the carbohydrate/protein interactions that mediate biological processes clearly remains a major challenge in glycoscience. To address this issue and discover new bioactive molecules, extensive multidisciplinar research programs involving both glycobiology and chemistry have been developed over the past decade.[1] Unlike monovalent interactions that are weak and unspecific, it was clearly demonstrated that high selectivity and strong binding enhancement arise from multi-point contacts between clusters of glycans and proteins.[2] This so-called 'glycoside cluster effect' has deeply inspired the development of synthetic molecules incorporating covalently bound clusters of carbohydrates (glycoclusters) that either mimic or inhibit recognition processes involving bacterial toxins and vegetal or animal lectins,[3] sometimes with subnanomolar affinities.[4] Interestingly, other studies focusing more on the recognition processes have notably clarified the mechanistic parameters that may occur through chelating, proximity/statistical or clustering effects, depending on the tridimensional structures of both glycocluster and target protein.[5] While giving useful guidelines, these findings also clearly highlighted that an ideal system for amplified binding remains extremely difficult to design.

Optimization of the biological potency of bio-recognizable glycoclusters closely depends on the number of carbohydrate copies as well as their architecture. To this end, a large variety of synthetic glycoclusters displaying variable topology, valency and density has been explored so far. The typical approach to preparing such glycoconjugates consists of grafting carbohydrates onto either rigid or flexible backbones such as polymers,[6] calixarenes,[7] cyclodextrins,[8] peptide dendrimers,[9] poly(amidoamine) (PAMAM) dendrimers,[10] cyclopeptides,[11] oligonucleotides,[12] fullerenes[13] or nanoparticles.[14] However, tuning the glycocluster's structure is still faced with inherent difficulties that result from the difficulties in synthesising (*i.e.* chemical incompatibility, regio- and stereoselectivity, incomplete reactions, purifications) and structurally characterising highly glycosylated molecules.

As part of a long-term program to design new bioactive glycoconjugates, we previously reported a first generation of conformationally stable cyclopeptide scaffolds, namely Regioselectively Addressable Functionalized Templates (RAFTs),[11,15] whose lysine side chains of one addressable domain were decorated with four

[a]*Département de Chimie Moléculaire, UMR CNRS 5250 and ICMG FR 2607, Université Joseph Fourier, BP53, 38041 Grenoble Cedex 9, France. E-mail: olivier.renaudet@ujf-grenoble.fr; Fax: +33 4 56 52 08 05; Tel: +33 4 56 52 08 33*

[b]*Institute of Microbiology, Academy of Sciences of the Czech Republic, Vídeňská 1083, CZ-14220 Praha 4, Czech Republic. E-mail: kren@biomed.cas.cz; Fax: +42 0296442509; Tel: +42 0296442510*

† Electronic supplementary information (ESI) available: Sample preparation for MALDI-TOF-MS analysis, analytical data for compounds **7**, **8**, **9**, **10**, **11**, **12**, RK-CHO_{16}, **18**, **19**, **20**, **21**, stability of compound **15** and inhibition curves of ELLA test with ConA. See DOI: 10.1039/c0ob00772b

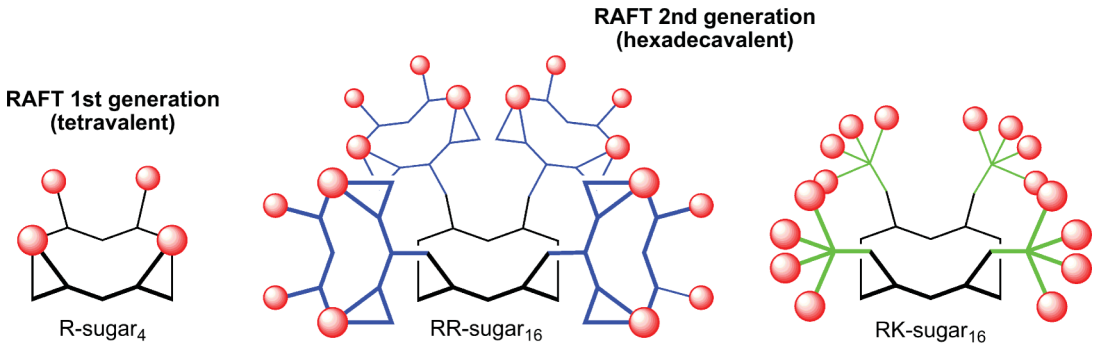

Fig. 1 General structure of the first and the second generation of cyclopeptide-based glycoclusters.

copies of either identical[16] or different glycans.[17] Depending on the expected biological application, the incorporation of additional lysine(s) into the cyclopeptide sequence allowed the second addressable domain to be functionalised. Some compounds were thus proved to be very effective immunoactive compounds,[18] albeit exhibiting lectin binding with only modest affinities.[16,19] In order to improve the recognition properties of those cyclopeptide-based glycoclusters towards lectins in particular, we were interested in the present study to develop new generations of compounds with higher glycosidic valency, density and various levels of rigidity. By analogy to the divergent strategy employed for glycodendrimer fabrication,[10a,20] here we report a modular chemoselective strategy to iteratively introduce either a flexible polylysine framework or a constrained cyclopeptide onto a RAFT core, thus providing two different hyperbranched skeletons in a controlled manner (Fig. 1). Biologically relevant carbohydrates were next conjugated to obtain new series of glycodendrimer-like structures, namely dendri-RAFTs "RK-sugar$_{16}$" (*i.e.* with the RAFT-polylysine core) and "RR-sugar$_{16}$" (*i.e.* with the RAFT-RAFT core). The efficiency of the assembly process was demonstrated through the preparation of dendri-RAFTs incorporating sixteen copies of βGal, αMan, βLac or Thomsen–Freidenreich (αTF) cancer antigen that were characterized by bi-dimensional NMR experiments, mass spectrometry and probed with a model lectin.

Results and discussion

Synthesis of dendri-RAFTs

In this study, we selected an oxime-based strategy which has proved to be perfectly suitable for the stepwise construction of complex macromolecules, as shown in a wide range of biological applications.[21] This approach consists of a chemoselective condensation between oxyamine- and aldehyde-containing molecules. For the preparation of glycoconjugates,[22] free reducing glycans were covalently coupled to oxyamine-containing compounds without a prior activation step. Depending on the nature of both oxyamino derivative and glycan, the resulting glycoconjugates were either obtained as an open-chain oxime or as a mixture of α/β pyranose/furanose neoglycosides in a molecular ratio that remains difficult to control.[23] Alternatively, an efficient phase-transfer catalysis procedure to stereoselectively incorporate the β-oxyamine group at the anomeric carbon was described.[24] The resulting glycosylhydroxylamines offer the advantages of being highly reactive with aldehyde- or ketone-containing molecules,[25] and more importantly of presenting a pre-defined anomer configuration that is not affected during its conjugation. In our laboratory, we extended the latter strategy by developing an efficient synthetic route to prepare both oxyamino α- and β-glycosyls from the corresponding glycosyl fluorides.[26] We thus applied this methodology to a series of carbohydrate recognition motifs *i.e.* βGal **1**,[27] αMan **2**,[28] βLac **3**[28] and the cancer-related antigen αTF **4**,[29] which were obtained in 5 to 16 steps then successively conjugated to aldehyde-containing scaffolds using oxime ligation (Fig. 2).

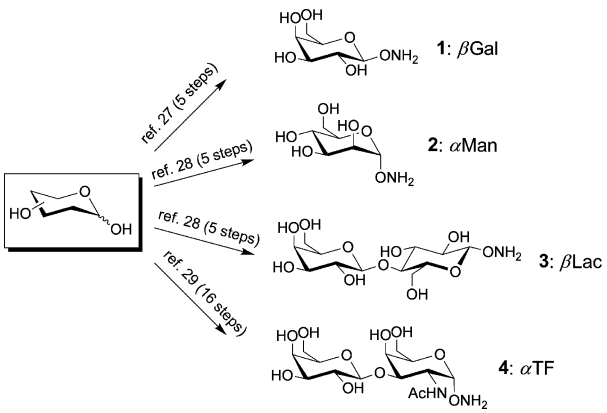

Fig. 2 Structure of oxyamino-glycosyls **1**–**4**.

RR series. As mentioned above in the introduction, we designed a second generation of glycocyclopeptides by introducing various multivalent peptide skeletons onto the RAFT core in a multistep divergent strategy. Starting from the RAFT-containing aldehyde **5** described earlier,[30] we first selected a second RAFT molecule **6**[18e] containing an oxyamine functional group on one addressable domain, whereas four serine residues were used as masked aldehydes on the second domain (Scheme 1).

The ligation was performed in an aqueous buffer containing trifluroracetic acid (TFA) instead of acetic acid, which was found to react in certain cases with oxyamine groups to form the corresponding hydroxamic esters. The expected conjugate **7** was thus obtained in 0.1% TFA in H_2O at 37 °C after 4 h with a quantitative conversion ratio, as proved by HPLC analysis (see the ESI†). In order to avoid time-consuming preparative HPLC to remove the excess of **6**, its oxyamine group was simply quenched with acetone to render this compound unreactive in the next step. Aldehyde groups were next generated from **7** by

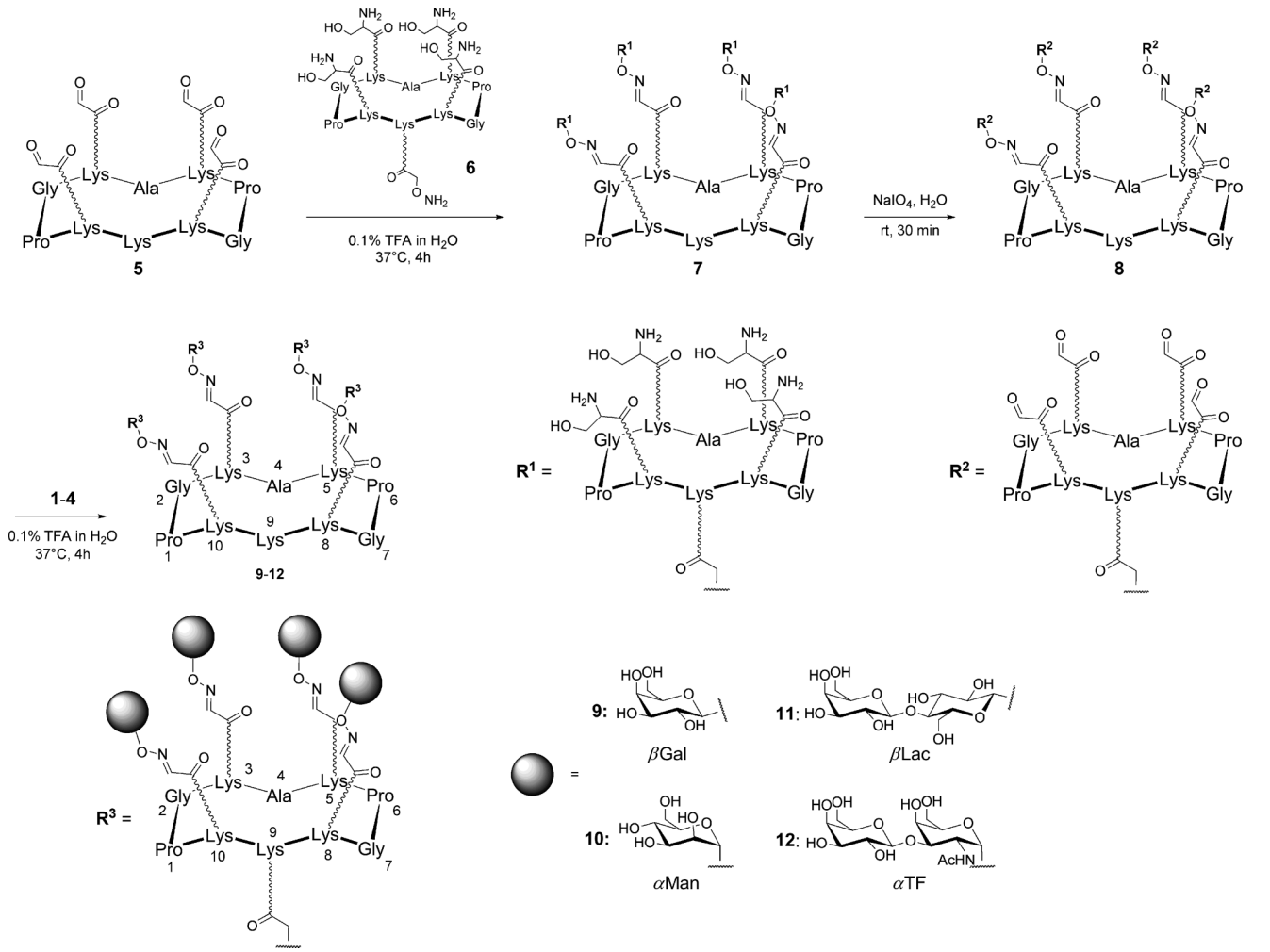

Scheme 1 Divergent strategy for the preparation of the hexadecavalent dendri-RAFTs RR-sugar$_{16}$ **9–12**.

the addition of sodium periodate[31] in the previous crude reaction mixture. This one-pot procedure gave the resulting compound **8** containing sixteen aldehyde groups after 30 min and semi-preparative HPLC, with an excellent yield (92%) and purity. Whereas electrospray ionisation mass spectrometry (ESI) detected the expected multicharged ions for this compound, the ^{1}H NMR spectrum recorded at 400 MHz in D_2O contained a signal at 5.33 ppm that showed that all sixteen aldehyde groups were present in the hydrate form (see the ESI†). We finally generated a series of four original RR-sugar$_{16}$ glycoclusters varying in their sugar head group. They were prepared from **8** under the oxime coupling conditions described previously using a 10-fold excess of oxyamino glycosyls **1–4** to ensure complete cluster formation. The excess of free carbohydrate derivative was finally removed by semi-preparative HPLC purification, producing the hexadecavalent RR-sugar$_{16}$ **9–12** in yields ranging from 65 to 88%. Despite steric hindrance generated during the molecular assembly, HPLC traces showed crude mixture without trace of truncated fragment in each case, thus demonstrating the efficiency of our synthetic approach.

As another alternative, we investigated a convergent rather than divergent assembly strategy to assemble mannosylated glycocluster **10** as illustrated in Scheme 2. In this case, tetravalent glycocluster **13** was first prepared by oxime condensation between **5** and oxyamino mannosyl **2**. The side chain of the central lysine was next functionalized with oxyamino linker **14**[32] that was successively deprotected by treatment under mild acidic conditions to yield **15**. Surprisingly, oxime conjugation between this mannosylated glycocluster **15** and **5** to generate the RR-αMan$_{16}$ **10** failed under standard ligation conditions. In contrast with the crude mixture of **10** previously obtained using the divergent protocol, HPLC analysis here gave an unclean chromatogram (see the ESI†), suggesting that side reactions might occur during the oxime ligation. Whereas oxime linkages are well-known to be stable under mild acidic conditions, even in the presence of a large excess of oxyamino derivative,[33] we presume that this problem is certainly due to the presence of the oxyamine function in the oxime-containing molecule **15** itself, which could promote an intra- or intermolecular *trans*-oximation side reaction. Unfortunately, mass analysis of the reaction mixture did not find any signal to confirm or exclude this hypothesis. Therefore, this result showed this convergent approach to be completely unsuitable for the construction of dendri-RAFTs and prompted us to discard it.

RK series. A second class of hexadecavalent dendri-RAFT RK-sugar$_{16}$ was then prepared. In this series, a branched polylysine skeleton was attached onto the central RAFT core **16** to provide

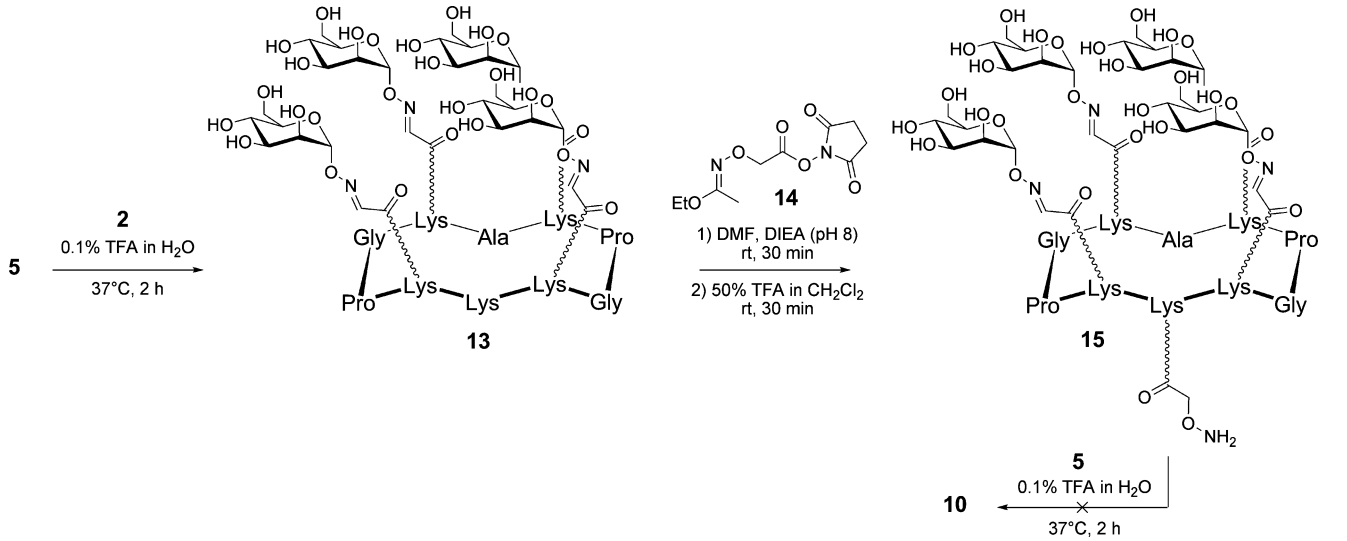

Scheme 2 Unsuccessful convergent strategy for the preparation hexadecavalent mannosyl cluster **10** from **15**.

higher flexibility than in the previous RR-sugar$_{16}$ series, in which a conformationally constrained cyclopeptide was used for carbohydrate presentation. A similar divergent approach including successive periodate oxidation and oxime ligation was thus followed for the construction of these RK-sugar$_{16}$ derivatives (Scheme 3). The aldehyde-containing molecule **16**[16] was first conjugated with the polylysine dendrimer **17**[32] in 0.1% TFA in H_2O. After 4 h at 37 °C, HPLC analyses showed pure crude reaction mixtures and complete conversion of **16** into the corresponding conjugate. This compound was consecutively oxidized with sodium periodate to yield a dendrimeric skeleton containing sixteen aldehydes, as confirmed by ESI and NMR experiments. The resulting compound was finally glycosylated with oxyamino glycosyls **1–4**, thus producing RK-sugar$_{16}$ glycoclusters in yields of 69–82% after HPLC purification. As for the construction of the RR-sugar$_{16}$ series, the coupling reactions with sugars occurred cleanly and no trace of undesired products due to *trans*-oximation side reaction or partial conjugation was observed by analytical HPLC.

Glycocluster characterization

One major limitation of the construction of complex macromolecules resides not only in the steric hindrance created during stepwise synthesis, but also in characterization difficulties using both NMR spectroscopy and mass spectrometry. This problem is intensified with large molecules containing multiple glycosylation sites such as glycoproteins.[34] Due to their high molecular weight (7.6–12.5 kDa) and carbohydrate density, our dendri-RAFTs were found to be subject to similar characterisation difficulties.

Final coupling assessment. While the expected number of aldehyde groups was confirmed with ^{1}H NMR spectroscopy and ESI spectrometry, the completeness of the final glycosylation had to be ascertained, since partial defects could presumably be difficult to detect.[10a] To confirm reaction completion, high-field NMR spectroscopy experiments were performed in D_2O. While the low structural symmetry of both series of dendri-RAFTs **9–12** and **18–21** strongly complicate the signals' resolution and multiplicity in the ^{1}H NMR spectra, COSY experiments enabled the unambiguous assignment of characteristic signals that correspond to the anomeric and oxime protons. For each compound, the integration of both signals (20 oxime protons and 16 anomer protons) was in perfect agreement with the presence of 16 sugar head groups.

^{1}H NMR resonance assignments. Complete bidimensional NMR studies were next performed for mannosylated compounds **10** and **19**. NMR data revealed a four-fold pseudo-symmetry that resulted in an equivalent magnetic environment for symmetry-related protons and, therefore, a dramatic degeneration of chemical shifts. This was particularly true for compound **10**, for which only one cyclodecapeptide is observable. The individual spin systems of peptide fragments were assigned based on an analysis of through-space nuclear Overhauser effect (NOESY) and through-bond correlated (DQF-COSY, TOCSY) spectra using well-established sequential strategy methods.[35] Nonpeptidic amide bonds, *e.g.* between two lysines *via* an oxime linker, were confirmed by visualising NOE correlations from the NHξ proton of the lysine side chain and the N=CH or the CH_2O protons of the oxime bond (Fig. 3). The assigned resonances are given in Table 1 for compound **10** and in Table 2 for compound **19**.

Structural calculations. While symmetry degeneration greatly simplifies resonance assignment, structure calculations are more complicated, since it becomes difficult to distinguish intramolecular correlations from intermolecular ones. However, distance constraints were unambiguously determined for both compounds, particularly between two lysines linked by their side chains, hence allowing correct orientation of the oxime bond. Models of the solution structures were obtained and are represented in Fig. 4. For more clarity, the four dendritic arms highlighted in yellow were spread widely. The resulting molecular models clearly show interesting differences, albeit showing similar size. Firstly, the cluster of sugars in RR-αMan$_{16}$ **10** appears more rigid and constrained than in **19**, presumably because the cyclopeptide skeleton prevents flexibility. In contrast the structure of the second RK-αMan$_{16}$ **19** is apparently much more flexible due to the presence of the polylysine core. Secondly, even if the number of

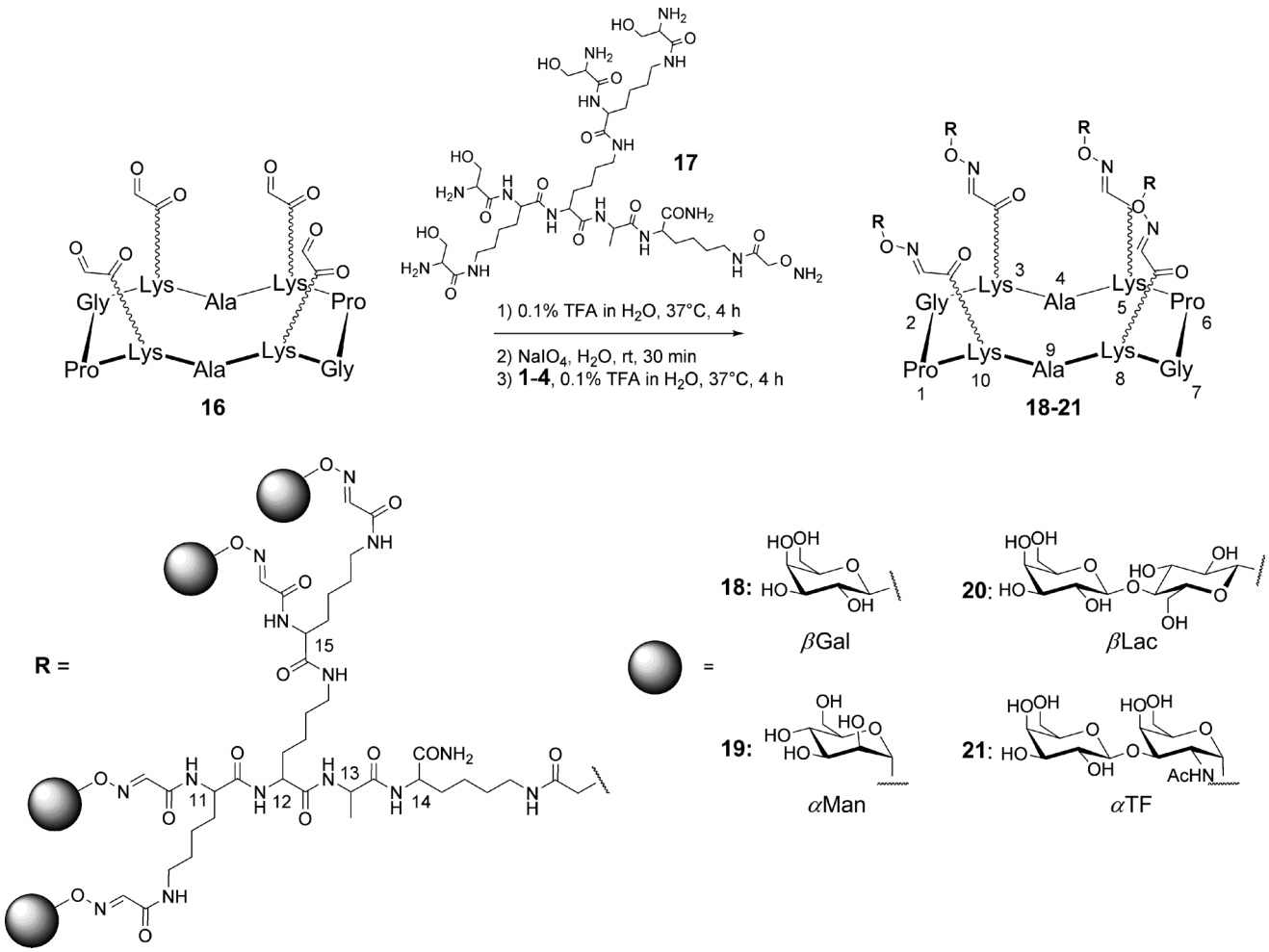

Scheme 3 Divergent strategy for the preparation of the hexadecavalent dendri-RAFTs RK-sugar$_{16}$ **18–21**.

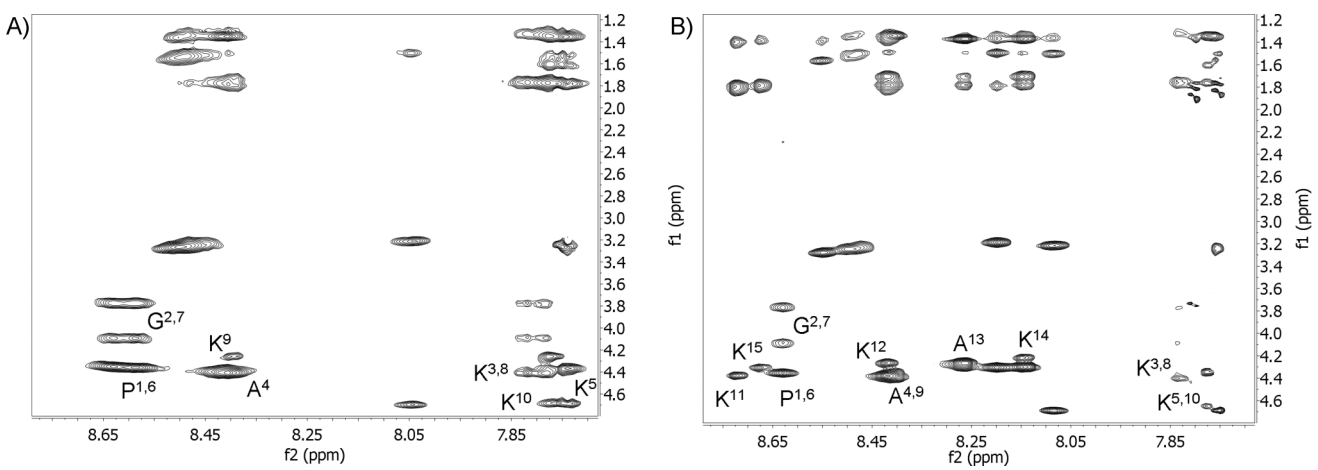

Fig. 3 Expanded regions of NOESY spectra (500 MHz) in a 95% H_2O/5% D_2O mixture showing NH-α and NH-side chain correlations. A) RR-αMan$_{16}$ **10**; B) RK-αMan$_{16}$ **19**. Residue numbering is given in Scheme 1 and 2, respectively.

mannosyl derivatives is identical in both molecules, the cluster density seems to be rather different, as shown by the sugar distribution onto the scaffold. The maximal distance between sugar moieties, that represents the upper distance limits, can indeed be estimated to be approximately 80 Å and 70 Å for RR-αMan$_{16}$ **10** and RK-αMan$_{16}$ **19**, respectively, whereas the sugars appear closer to each other in RR-αMan$_{16}$ **10**. We presume that these differences in both cluster rigidity and carbohydrate presentation might impact on their recognition properties with lectins.

Table 1 Proton chemical shift assignments for compounds RR-αMan$_{16}$ **10**[a]

Residue[b]	HN	Hα	Hβ	Hγ	Others
Pro-1,6		4.36	2.03, 2.31	1.97, 2.11	$CH_2\delta$ 3.66, 3.84
Gly-2,7	8.64	3.78, 4.09			
Lys-3,8	7.83	4.40	1.80	1.33	$CH_2\delta$ 1.53; $CH_2\varepsilon$ 3.28; NHξ 8.53
Ala-4	8.45	4.38	1.36		
Lys-5	7.78	4.67	1.65, 1.79	1.40	$CH_2\delta$ 1.56; $CH_2\varepsilon$ 3.29; NHξ 8.50
Lys-9	8.43	4.26	1.78	1.38	$CH_2\delta$ 1.52; $CH_2\varepsilon$ 3.24; NHξ 8.08
Lys-10	7.80	4.68	1.63, 1.78	1.36	$CH_2\delta$ 1.53; $CH_2\varepsilon$ 3.29; NHξ 8.53
CH_2–O-ox	4.70				
N═CH-ox	7.76, 7.79				
αMan	5.53 (H1)	4.14 (H2)	3.81 (H3)	3.65 (H4,5)	3.76, 3.84 (H6a, H6b)

[a] Proton assignments are in H_2O at 25 °C. [b] Residue numbering is given in Scheme 1.

Table 2 Proton chemical shift assignments for compounds RK-αMan$_{16}$ **19**[a]

Residue[b]	HN	Hα	Hβ	Hγ	Others
Pro-1,6		4.37	2.03, 2.30	2.02, 2.08	$CH_2\delta$ 3.64, 3.83
Gly-2,7	8.63	3.77, 4.09			
Lys-3,8	7.83	4.40	1.75, 1.78	1.36	$CH_2\delta$ 1.51; $CH_2\varepsilon$ 3.24; NH 8.47
Ala-4,9	8.41	4.36	1.35		
Lys-5,10	7.78	4.65	1.62, 1.75	1.36	$CH_2\delta$ 1.53; $CH_2\varepsilon$ 3.25; NHξ 8.49
Lys-11	8.72	4.38	1.81	1.40	$CH_2\delta$ 1.56; $CH_2\varepsilon$ 3.28; NHξ 8.56
Lys-12	8.42	4.26	1.79	1.36	$CH_2\delta$ 1.50; $CH_2\varepsilon$ 3.19; NHξ 8.21
Ala-13	8.27	4.27	1.37		
Lys-14	8.14	4.22	1.70, 1.78	1.37	$CH_2\delta$ 1.50; $CH_2\varepsilon$ 3.08; NHξ 8.22
Lys-15	8.67	4.31	1.79	1.38	$CH_2\delta$ 1.56; $CH_2\varepsilon$ 3.28; NHξ 8.60
CH_2–O-ox	4.69				
N═CH-ox	7.76, 7.80				
αMan	5.53 (H1)	4.12 (H2)	3.81 (H3)	3.63 (H4,5)	3.77, 3.85 (H6a, H6b)

[a] Proton assignments are in H_2O at 25 °C. [b] Residue numbering is given in Scheme 2.

MALDI-TOF characterization. While the peptide intermediates and the first generation of tetravalent glycoclusters reported previously[16,18] were easily analysed by routine ESI, direct mass analysis of these dendri-RAFTs compounds failed using similar ESI procedures. This difficulty can certainly be attributed to the presence of only one free lysine side-chain in dendri-RAFTs **9–12**, whereas dendri-RAFTs **18–21** contain no protonation site. In addition, together with the presence of salts, the well-known fragmentation of oxime linkages observed by a tandem quadrupole time-of-flight mass spectrometer with electrospray ion source (ESI-QqTOF)[36] might cause a distribution of the molecular ion signals between several species, thus precluding any signal detections. Therefore, we expected that matrix-assisted laser desorption/ionization, time-of-flight mass spectrometry (MALDI-TOF-MS) experiments would give better results. Despite inherent difficulties associated with the MALDI detection of glycopeptides, it was demonstrated that a suitable choice of parameters, including the desorption matrix, sample preparation, pH and instrumental conditions can significantly improve the analysis of glycoconjugates.[37]

Their average molecular weight was thus successfully determined by MALDI-TOF. To perform these analyses, sample pretreatment in an OligoR3 microcolumn using a pH 8.1, 100 mM ammonium acetate buffer and 2,5-dihydroxybenzoic acid as the MALDI matrix was necessary to yield MALDI-TOF positive spectra in linear mode. We thus obtained clean mass spectra showing the expected molecular peak for each glycocluster with partial fragmentation. All samples revealed a m/z signal of $[M+Na]^+$ except for dendri-RAFT RK-αTF$_{16}$ **21**, which interestingly produced a $[M+Na_2]^+$ molecular ion when applying the same experimental approach prior to MS analysis (Table 3).

On the other hand, the use of POROS 20 R2 (Applied Biosystems, CA, USA) or Carbograph (Grace, IL, USA) resin and also various washing protocols (0.1% ammonia solution, 0.1% ammonium acetate without pH adjustment, pure water, 0.1% acetic acid or 0.1% trifluoroacetic acid instead of pH 8.1, 100 mM ammonium acetate buffer) provided no or very poor MS signals. Based on optimization experiments on the pre-cleaning method, we can conclude that not only the type of chromatography resin but also type of washing buffer used and its pH strongly affected the obtained MS data. However, it should be mentioned that the sample RR-αTF$_{16}$ **12** did not produce any MS signal whatever the method.

Biological evaluation of mannosylated dendri-RAFT with ConA

To probe the binding properties of our dendri-RAFT, we chose a model lectin from *Canavalia ensiformis* (ConA) whose mannose binding sites are separated by about 65 Å, hence appearing suitable for multivalent interactions with our glycoclusters. Hexadecavalent dendri-RAFTs RR-αMan$_{16}$ **10** and RK-αMan$_{16}$ **19** were tested and compared with the tetravalent mannosylated compound R-αMan$_4$ **13** using Enzyme-Like Lectin Assays (ELLA).[38] Methyl α-D-mannopyranoside was used as monovalent reference.

Table 3 MALDI-TOF MS analysis of RR-sugar$_{16}$ **9–12** and RK-sugar$_{16}$ **18–21**[a]

Compound	Formula	Calculated average mass	Experimental mass	Error (ppm)
RR-βGal$_{16}$ **9**	$C_{379}H_{605}N_{95}O_{174}Na$	9299.4983	9297.7	165
RR-αMan$_{16}$ **10**	$C_{379}H_{605}N_{95}O_{174}Na$	9299.4983	9298.0	161
RR-βLac$_{16}$ **11**	$C_{475}H_{765}N_{95}O_{254}Na$	11893.7767	11892.5	107
RR-αTF$_{16}$ **12**	$C_{507}H_{813}N_{111}O_{254}O_{254}$		*not detected*	
RK-βGal$_{16}$ **18**	$C_{296}H_{482}N_{74}O_{154}Na$	7564.4792	7563.4	142
RK-αMan$_{16}$ **19**	$C_{296}H_{482}N_{74}O_{154}Na$	7564.4792	7563.7	103
RK-βLac$_{16}$ **20**	$C_{392}H_{642}N_{74}O_{234}Na$	10158.7576	10156.9	183
RK-αTF$_{16}$ **21**	$C_{424}H_{690}N_{90}O_{234}$ Na_2	10838.5883	10836.5	192

[a] MALDI-TOF MS data were obtained in 2,5-dihydroxybenzoic acid matrix and all samples revealed a signal of $[M+Na]^+$, except the sample RK-αTF$_{16}$ **21** which provided a $[M+Na_2]^+$ using the approach described in the Experimental Section. The sample RR-αTF$_{16}$ **12** did not reveal any MS signal.

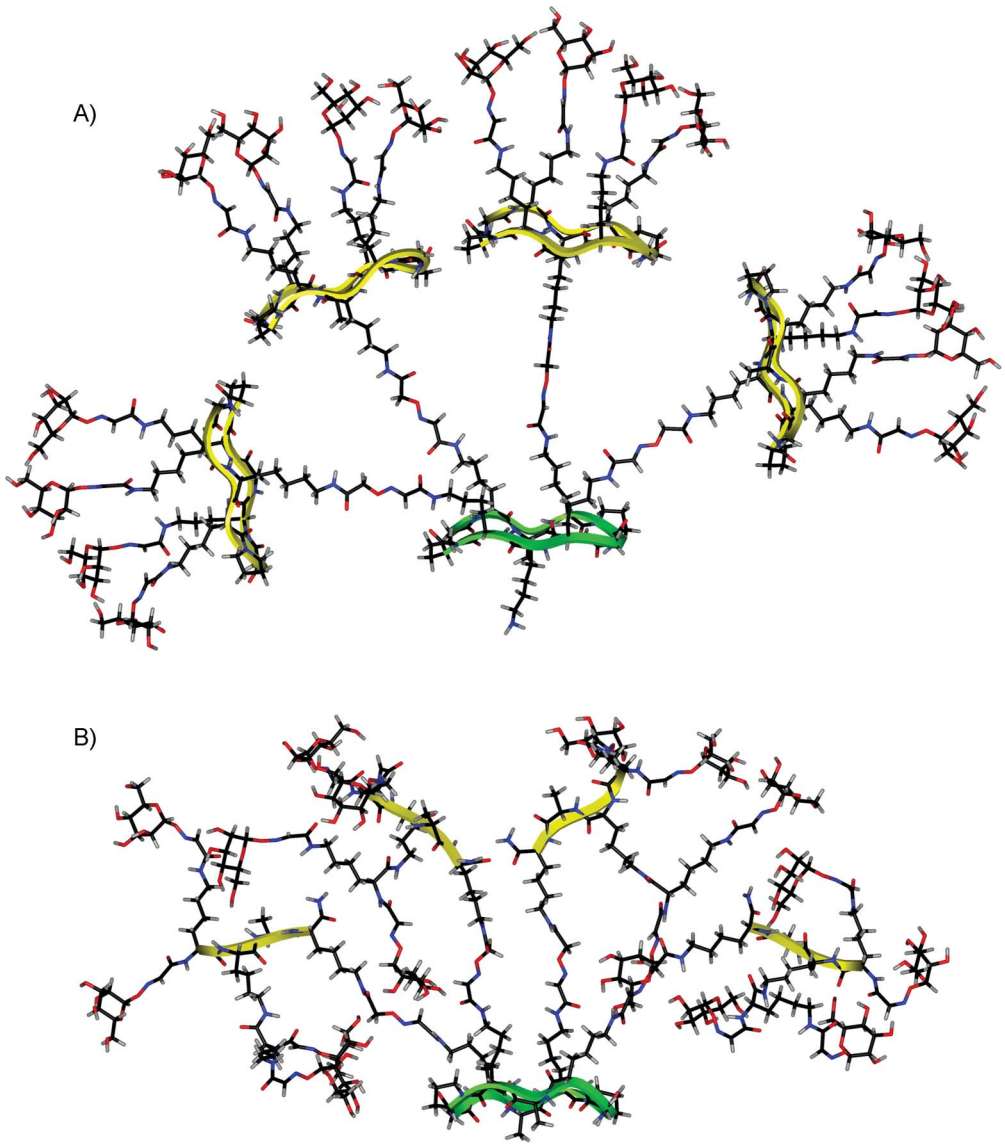

Fig. 4 Molecular modelling of: A) RR-αMan$_{16}$ **10**; B) RK-αMan$_{16}$ **19**.

This experiment measured the ability of serially diluted glycoclusters to inhibit the binding between ConA labelled with horseradish peroxidase (HRP) and a polymeric mannosylated ligand (PAA-αMan) immobilized on the microtiter well. We thus obtained an IC_{50} value that corresponds to the concentration necessary for 50% inhibition and is assumed to be proportional to the corresponding binding affinities.

As summarized in Table 4, the tetravalent compound R-αMan$_4$ **13** exhibited a modest IC_{50} (58 μM), which was only slightly better than the methyl-α-D-mannopyranoside (199 μM). Indeed,

Table 4 ELLA data for binding inhibition of ConA-HRP with mannosylated glycoclusters[a]

Compound	n[b]	IC_{50}/μM	Rel. pot.[c]	Rel. pot./sugar[d]
αManOMe	1	199	1.0	1.0
R-αMan_4 **13**	4	58	3.4	0.8
RR-αMan_{16} **10**	16	3.6	55.3	3.4
RK-αMan_{16} **19**	16	0.7	284	17.7
RR-βGal_{16} **9**	16	No inhibition	—	—

[a] Each experiment was performed in triplicate. [b] Number of sugar units in the ligand. [c] Relative potency = IC_{50}(αManOMe)/IC_{50}(dendrimer). [d] Relative potency/sugar = relative potency/n.

this result is in perfect agreement with previous fluorescence anisotropy[16] and SPR[19c] studies showing that the multivalent effect of this tetravalent glycocluster is almost negligible with ConA. More interestingly, inhibitory potencies were obtained with hexadecavalent RR-αMan_{16} **10** (IC_{50} 3.6 μM), whereas the most significant effect was observed with RK-αMan_{16} **19** (IC_{50} 0.7 μM). Their relative inhibitory potencies were 55 and almost 300 times better than methyl-α-D-mannopyranoside, respectively. When the relative potencies were expressed in terms of the number of mannoside residues in each hexadecavalent molecule, the level of inhibition was 3.4- and 17.7-fold higher with compounds **10** and **19**, respectively. Taken together, these results clearly indicate that a multivalent effect is occurring in the presence of a hexadecavalent structure, in particular with compound **19**. It should also be mentioned that RR-βGal_{16} **9** was evaluated as the negative control, since galactosylated ligands do not bind to ConA. No inhibition was observed with this compound. This confirms that inhibitory effects can be attributed to the mannose headgroup and its presentation instead of the dendritic skeleton itself.

Conclusions

A new generation of structurally diverse glycoclusters was described and studied in this paper. Two series of dendri-RAFTs composed of polylysine (RK series) or cyclopeptide (RR series) skeletons attached to a central cyclopeptide platform were designed and synthesized in a controlled manner using an efficient divergent protocol. Both families provided sixteen anchoring sites that were easily functionalized by oximation with several carbohydrate moieties, those being βGal, αMan, βLac or cancer-related Thomsen–Freidenreich (TF). We thus obtained novel hexadecavalent dendri-RAFTs differing in their spatial arrangement and glycosidic density as shown by NMR spectroscopy and structural calculations. Despite being heavily glycosylated, these compounds were next treated using an optimized pre-cleaning protocol that allowed their unambiguous structural characterization by MALDI-TOF-MS. It should be mentioned that the oxime instability observed during MS analyses, in particular under highly acidic conditions, does not preclude the utilization of oxime-containing compounds *in vitro* and *in vivo*.[39] To evaluate their binding properties, preliminary recognition assays were finally performed with the model lectin ConA. In comparison with the mannosylated tetravalent structure **13**, which showed negligible multivalent interaction with ConA, hexadecavalent structures exhibited a significant binding improvement, in particular with RK-αMan_{16} **19**. This result clearly confirms that not only the carbohydrate copy number, but also the tridimensional structure of the glycocluster affects its recognition properties. Although these hexadecavalent compounds only differ in their peptide skeleton, the higher inhibition potency induced by **19** might indeed be explained by the higher degree of freedom of carbohydrates and a suitable distribution for multivalent interaction. Together with the efficiency of both assembly and characterization protocols, these results clearly showed interesting recognition properties that pave the way to the development of relevant biological applications. In particular, intensive research towards the design of potent inhibitors capable of blocking the early stage of pathogen infections is currently underway in our laboratory.

Experimental

Materials and general procedures

All chemical reagents were purchased from Aldrich (Saint Quentin Fallavier, France) or Acros (Noisy-Le-Grand, France) and were used without further purification. Protected amino acids and Fmoc-Gly-Sasrin resin were obtained from Advanced ChemTech Europe (Brussels, Belgium), Bachem Biochimie SARL (Voisins-Les-Bretonneux, France) and France Biochem S.A. (Meudon, France). PyBOP was purchased from France Biochem. HRP-labelled Concanavalin A (ConA-HRP), Bovine Serum Albumin (BSA), methyl α-D-mannopyranoside and SIGMA *FAST* OPD were purchased from Sigma-Aldrich. Polymeric α-D-mannose (PAA-α-D-Man) was obtained from Lectinity Holding, Inc., Moscow. Optical density was measured with a microtiter plate reader (SPECTRAmax, model PLUS384, Molecular Devices). Reaction progress was monitored by reverse-phase HPLC on Waters equipment using C_{18} columns. Analytical and preparative separation was carried out at 1.3 mL min^{-1} (Nucleosil 120 Å 3 μm C_{18} particles, 30 × 4.6 mm^2) and at 22 mL min^{-1} (Delta-Pak 300 Å 15 μm C_{18} particles, 200 × 25 mm^2) with UV monitoring at 214 nm and 250 nm using a linear A–B gradient (buffer A: 0.09% CF_3CO_2H in water; buffer B: 0.09% CF_3CO_2H in 90% acetonitrile). Each intermediate peptide was analyzed by mass spectrometry using electrospray ionization on a VG Platform II in positive mode. Mass spectra for hexadecavalent glycoclusters were acquired on a Bruker-Daltonics MALDI-TOF/TOF UltraFlex III (linear mode) after sample pre-treatment in an OligoR3 microcolumn (Applied Biosystems, USA) using 2,5-dihydroxybenzoic acid as the matrix. ^1H NMR spectra were recorded in D_2O at 400 MHz with a Bruker Avance 400. TOCSY, DQF-COSY and NOESY for compounds **10** and **19** were obtained in 95% H_2O/5% D_2O at 500 MHz with a Varian Unity plus spectrometer.

Preparation of aldehyde scaffold RR-CHO_{16} (8)

A solution of R-CHO_4Lys **5** (5.7 mg, 4.0 μmol) and R-Ser_4ONH_2 **6** (48.2 mg, 24.0 μmol) was stirred at 37 °C in 0.1% TFA in H_2O (4 mL, v/v). After 4 h, analytical HPLC found the quantitative conversion of **5** into the RR-Ser_{16} **7**. Analytical HPLC: R_t: 5.5 min (gradient: 5 to 100% B in 15 min); ESI^+-MS: calcd. for $C_{299}H_{509}N_{95}O_{94}$ 6939.0, found: m/z 6940.5 $[M+H]^+$. After the addition of acetone (100 μL) to the crude reaction mixture, compound **7** was oxidized with sodium periodate (205 mg, 0.96 mmol) at room temperature. The crude mixture was finally purified by semi-preparative HPLC after 1 h to obtain the

aldehyde-containing peptide RR-CHO_{16} **8** (25 mg, 92%). Analytical RP-HPLC: R_t: 5.8 min (gradient: 5 to 100% B in 15 min); semi-preparative HPLC: R_t: 15.0 min (gradient: 5 to 60% B in 30 min); ESI$^+$-MS: calcd. for $C_{283}H_{429}N_{79}O_{94}$ 6442.0, found: *m/z* 6460.3 $[M+H_2O]^+$; ^{1}H NMR (400 MHz, D_2O): δ = 7.82–7.77 (m, 4 H, 4×Hox), 5.33–5.31 (m, 16 H, 16×$CH(OH)_2$), 4.77–4.73 (m, 8 H, 4×CH_2O), 4.50–4.33 (m, 30 H, 30×H_α), 4.16 (d, 10 H, $^2J_{H\alpha,H\alpha'}$ = 17.7 Hz, 10×$H_{\alpha Gly}$), 3.94–3.78 (m, 20 H, 10×$H_{\alpha' Gly}$ and 10×$H_{\delta pro}$), 3.76–3.67 (m, 10 H, 10×$H_{\delta' Pro}$) 3.36–3.18 (m, 48 H, 24×$CH_{2\varepsilon Lys}$), 3.04 (t, 2 H, $^3J_{H\varepsilon,H\delta}$ = 7.7 Hz, $CH_{2\varepsilon Lys}$), 2.30–2.41 (m, 10 H, 10×$H_{\beta Pro}$), 2.20–1.30 (m, 205 H).

Preparation of hexadecavalent RR-sugar$_{16}$ (9)–(12)

RR-βGal$_{16}$ (9). The aldehyde-containing peptide **8** (4.0 mg, 0.58 μmol) was dissolved in 0.1% TFA in H_2O (0.6 mL, v/v) and βGal **1** (3.6 mg, 18.5 μmol) was added to the mixture which was stirred at 37 °C. After 4 h, semi-preparative HPLC of the crude mixture yielded the hexadecavalent galactosyl cluster **9** (4.5 mg) in an 82% yield. Analytical RP-HPLC: R_t: 5.6 min (gradient: 5 to 100% B in 15 min); semi-preparative HPLC: R_t: 12.6 min (gradient: 5 to 60% B in 30 min); δ = 7.88–7.78 (m, 20 H, 20×Hox), 5.18–5.12 (m, 16 H, 16×H1), 4.49–4.29 (m, 30 H, 30×H_α), 4.15 (d, 10 H, $^2J_{H\alpha,H\alpha'}$ = 17.6 Hz, 10×$H_{\alpha Gly}$), 4.05–4.02 (m, 16 H, 16×H4), 3.93–3.65 (m, 110 H, 16×H2, 16×H3, 16×H5, 32×H6, 10×$H_{\alpha' Gly}$, 20×$CH_{2\delta pro}$), 3.38–3.23 (m, 48 H, 24×$CH_{2\varepsilon Lys}$), 3.04 (t, 2 H, $^3J_{H\varepsilon,H\delta}$ = 8.0 Hz, $CH_{2\varepsilon Lys}$), 2.41–2.30 (m, 10 H, 10×$H_{\beta Pro}$), 2.18–1.30 (m, 205 H); MALDI-TOF-MS (positive linear mode): calcd average mass for $C_{379}H_{605}N_{95}O_{174}$ 9276.508, found: *m/z* 9297.7 $[M+Na]^+$.

RR-αMan$_{16}$ (10). Compound **10** (6.0 mg, 88%) was obtained by following a similar procedure. Analytical HPLC: R_t: 5.7 min (gradient: 5 to 100% B in 15 min); semi-preparative HPLC: R_t: 13.1 min (gradient: 5 to 60% B in 30 min); ^{1}H NMR resonance assignments are given in Table 1; MALDI-TOF-MS (positive linear mode): calcd average mass for $C_{379}H_{605}N_{95}O_{174}$ 9276.508, found: *m/z* 9298.0 $[M+Na]^+$.

RR-βLac$_{16}$ (11). Compound **11** (4.7 mg, 68%) was obtained by following a similar procedure. Analytical RP-HPLC: R_t: 5.4 min (gradient: 5 to 100% B in 15 min); semi-preparative HPLC: R_t: 12.0 min (gradient: 5 to 60% B in 30 min); ^{1}H NMR (500 MHz, D_2O): δ = 7.89–7.77 (m, 20 H, 20×Hox), 5.27–5.21 (m, 16 H, 16×H1′), 4.76–4.74 (m, 8 H, 4×CH_2O), 4.52 (d, 16 H, $^3J_{1,2}$ = 7.7 Hz, 16×H1), 4.50–4.30 (m, 30 H, 30×H_α), 4.15 (d, 10 H, $^2J_{H\alpha,H\alpha'}$ = 17.6 Hz, 10×$H_{\alpha Gly}$), 4.06–3.96 (m, 36 H, 16×H4, 10×$H_{\alpha' Gly}$, 10×$H_{\delta pro}$), 3.94–3.75 (m, 138 H, 16×H3′, 16×H4′, 16×H5, 16×H5′, 32×H6, 32×H6′, 10×$H_{\delta' Pro}$), 3.72 (dd, 16 H, $^3J_{3,4}$ = 3.4 Hz, $^3J_{2,3}$ = 9.9 Hz, 16×H3), 3.67–3.58 (m, 32 H, 16×H2, 16×H2′), 3.38–3.22 (m, 48 H, 24×$CH_{2\varepsilon Lys}$), 3.04 (t, 2 H, $^3J_{H\varepsilon,H\delta}$ = 7.7 Hz, $CH_{2\varepsilon Lys}$), 2.42–2.30 (m, 10 H, 10×$H_{\beta Pro}$), 2.20–1.30 (m, 205 H); MALDI-TOF-MS (positive linear mode): calcd average mass for $C_{475}H_{765}N_{95}O_{254}$ 11870.7870, found: *m/z* 11892.5 $[M+Na]^+$.

RR-αTF$_{16}$ (12). Compound **12** (3.6 mg, 65%) was obtained by following a similar procedure. Analytical HPLC: R_t: 5.5 min (gradient: 5 to 100% B in 15 min); semi-preparative HPLC: R_t: 11.6 min (gradient: 5 to 60% B in 30 min); ^{1}H NMR (500 MHz, D_2O): δ = 7.83–7.78 (m, 20 H, 20×H_{ox}), 5.64–5.60 (m, 16 H, 16×H1′), 4.75–4.73 (m, 8 H, 4×CH_2O), 4.60–4.53 (m, 32 H, 16×H1, 16×H2′), 4.49–4.29 (m, 46 H, 16×H4, 30×H_α), 4.19–4.09 (m, 26 H, 16×H3′, 10×$H_{\alpha Gly}$), 4.05 (bt, 16 H, $^3J_{5',6'}$ = 6.0 Hz, 16×H5′), 3.97 (bd, 16 H, $^3J_{4,5}$ = 3.1 Hz, 16×H4), 3.87–3.64 (m, 126 H, 16×H3, 16×H5, 32×H6, 32×H6′, 10×$H_{\alpha' Gly}$, 20×$CH_{2\delta pro}$), 3.59 (bt, 16 H, $^3J_{1,2}$ = 7.8 Hz, 16×H2), 3.40–3.19 (m, 48 H, 24×$CH_{2\varepsilon Lys}$), 3.08–3.02 (m, 2 H, $CH_{2\varepsilon Lys}$), 2.39–2.27 (m, 10 H, 10×$H_{\beta Pro}$), 2.18–1.23 (m, 253 H); MALDI-TOF-MS (positive linear mode): no signal was detected.

Preparation of the aldehyde scaffold RK-CHO_{16}

The aldehyde-containing RK-CHO_{16} was prepared successively after oxime conjugation between R-CHO_4Ala_2 **16** (5.0 mg, 4.0 μmol) and polyKSer$_4$$ONH_2$ **17** (38.1 mg, 24.0 μmol) (RK-Ser$_{16}$: Analytical HPLC: R_t = 7.4 min (5 to 40% B in 15 min, λ = 214 and 250 nm); ESI$^+$-MS (positive mode): calcd for $C_{216}H_{386}N_{74}O_{74}$ 5203.9, found: *m/z* 5204.3 $[M+H]^+$) then oxidation with sodium periodate following the procedures described for **8**. Analytical HPLC: R_t = 8.3 min (5 to 40% B in 15 min, λ = 214 and 250 nm); semi-preparative HPLC: R_t: 13.6 min (gradient: 5 to 40% B in 30 min); ^{1}H NMR (400 MHz, D_2O): δ = 7.77–7.76 (m, 4 H, 4×H_{ox}), 5.34 (s, 8 H, 8×$CH(OH)_2$), 5.28 (s, 8 H, 8×$CH(OH)_2$), 4.75–4.68 (m, 8 H, 4×CH_2O), 4.40–4.20 (m, 28 H, 28×H_α), 4.12 (d, 2 H, $^2J_{H\alpha,H\alpha'}$ = 17.5 Hz, 2×$H_{\alpha Gly}$), 3.88–3.63 (m, 6 H, 2×$H_{\alpha' Gly}$, 2×$CH_{2\delta pro}$), 3.30–3.18 (m, 40 H, 20×$CH_{2\varepsilon Lys}$), 2.92–2.36 (m, 8 H, 2×$CH_{2\beta Pro}$, 2×$CH_{2\gamma Pro}$), 1.75–1.27 (m, 138 H); ESI$^+$-MS: calcd for $C_{200}H_{306}N_{58}O_{74}$ 4707.0; found: *m/z* 4707.8 $[M+H]^+$.

Preparation of hexadecavalent RK-sugar$_{16}$ (18)-(21)

RK-βGal$_{16}$ (18). Compound **18** (7.0 mg, 77%) was obtained by following the oxime ligation procedure described for **9**. Analytical HPLC: R_t = 8.0 min (5 to 40% B in 15 min, λ = 214 and 250 nm); semi-preparative HPLC: R_t: 12.4 min (gradient: 5 to 40% B in 30 min); ^{1}H NMR (500 MHz, D_2O): δ = 7.88–7.77 (m, 20 H, 20×H_{ox}), 5.15–5.12 (m, 16 H, 16×H1), 4.76–4.71 (m, 8 H, 4×CH_2O), 4.45–4.23 (m, 28 H, 28×H_α), 4.12 (d, 2 H, $^2J_{H\alpha,H\alpha'}$ = 17.8 Hz, 2×$H_{\alpha Gly}$), 4.03–3.99 (m, 16 H, 16×H4), 3.89–3.70 (m, 86 H, 16×H2, 16×H3, 16×H5, 32×H6, 2×$H_{\alpha' Gly}$, 2×$CH_{2\delta pro}$), 3.35–3.20 (m, 40 H, 20×$CH_{2\varepsilon Lys}$), 2.35–1.32 (m, 146 H); MALDI-TOF-MS (positive linear mode): calcd average mass for $C_{296}H_{482}N_{74}O_{154}$ 7541.4894, found: *m/z* 7563.4 $[M+Na]^+$.

RK-αMan$_{16}$ (19). Compound **19** (7.7 mg, 73%) was obtained by following the oxime ligation procedure described for **9**. Analytical HPLC: R_t = 8.4 min (5 to 40% B in 15 min, λ = 214 and 250 nm); semi-preparative HPLC: R_t: 13.6 min (gradient: 5 to 40% B in 30 min;); ^{1}H NMR resonance assignments are given in Table 2; MALDI-TOF-MS (positive linear mode): calcd average mass for $C_{296}H_{482}N_{74}O_{154}$ 7541.4894, found: *m/z* 7563.7 $[M+Na]^+$.

RK-βLac$_{16}$ (20). Compound **20** (10.0 mg, 82%) was obtained by following the oxime ligation procedure described for **9**. Analytical HPLC: R_t = 8.0 min (5 to 40% B in 15 min, λ= 214 and 250 nm); semi-preparative HPLC: R_t: 11.2 min (gradient: 5 to 40% B in 30 min); ^{1}H NMR (400 MHz, D_2O): δ = 7.91–7.79 (m, 20 H, 20×H_{ox}), 5.27–5.22 (m, 16 H, 16×H1′), 4.76–4.74 (m, 8 H, 4×CH_2O), 4.52 (d, 16 H, $^3J_{1,2}$ = 7.7 Hz, 16×H1), 4.47–4.26 (m, 28 H, 28×H_α), 4.07–3.96 (m, 34 H, 16×H6a′, 16×H4, 2×$H_{\alpha Gly}$), 3.93–3.75 (m, 118 H, 16×H3′, 16×H4′, 16×H5, 16×H5′, 16×H6b′, 32×H6′, 2×$H_{\alpha' Gly}$, 2×$CH_{2\delta pro}$), 3.73 (dd, 16 H, $^3J_{3,4}$ = 3.2 Hz, $^3J_{2,3}$ = 10.0 Hz, 16×H3), 3.68–3.59 (m, 32 H, 16×H2, 16×H2′), 3.37–3.24 (m, 40 H, 20×$CH_{2\varepsilon Lys}$), 2.36–1.27 (m, 146 H); MALDI-TOF-MS (positive

linear mode): calcd average mass for $C_{392}H_{642}N_{74}O_{234}$ 10135.7678, found: m/z 10156.9 $[M+Na]^+$.

RK-αTF$_{16}$ (21). Compound **21** (6.0 mg, 69%) was obtained by following the oxime ligation procedure described for **9**. Analytical HPLC: R_t = 7.9 min (5 to 40% B in 15 min, λ = 214 and 250 nm); semi-preparative HPLC: R_t: 12.0 min (gradient: 5 to 40% B in 30 min); ^{1}H NMR (500 MHz, D_2O): δ = 7.80–7.76 (m, 20 H, 20×H_{ox}), 5.62–5.59 (m, 16 H, 16×H1′), 4.73–4.69 (m, 8 H, 4×CH_2O), 4.56 (td, 16 H, $^3J_{1',2'}$ = 3.8, $^3J_{2',3'}$ = 11.5 Hz, 16×H2′), 4.51 (d, 16 H, $^3J_{1,2}$ = 7.6 Hz, 16×H1), 4.41–4.22 (m, 44 H, 16×H4′, 28×H_α), 4.15–4.07 (m, 18H, 16×H3′, 2×$H_{\alpha Gly}$), 4.02 (bt, 16 H, $^3J_{5',6'}$ = 6.0 Hz, 16×H5′), 3.93 (bd, 16 H, $^3J_{3,4}$ = 3.0 Hz, 16×H4), 3.83–3.62 (m, 102 H, 16×H3, 16×H5, 32×H6, 32×H6′, 2×$H_{\alpha'Gly}$, 2×$CH_{2\delta Pro}$), 3.58–3.52 (m, 16 H, 16×H2), 3.33–3.18 (m, 40 H, 20×$CH_{2\varepsilon Lys}$), 2.36–1.27 (m, 194H); MALDI-TOF-MS (positive linear mode): calcd average mass for $C_{424}H_{690}N_{90}O_{234}$ 10792.6088, found: m/z 10836.5 $[M+2Na]^+$.

NMR spectroscopy

Peptide samples were dissolved in a mixture of 95% H_2O/5% D_2O to a final concentration of 2–3 mM at 25 °C. A set of two-dimensional (2D) spectra, including TOCSY,[40] DQF-COSY[41] and NOESY[42] were acquired with 1.5 s steady state recovery time, mixing times (t_m) of 60 ms for TOCSY and 250 ms for NOESY. Water suppression was achieved by appending an excitation-sculpting module[43] to the non-selective detection pulse and with selective Gaussian-shaped pulses of 3–5 ms. The spin-lock mixing of the TOCSY experiment was obtained with a DIPSI-2[44] pulse train at $\gamma B_2/2\pi$ = 9–10 kHz. The acquisitions were performed over a spectral width of 10 ppm in both dimensions, with a matrix size of 2048 data points in t_2 and 256–512 points in t_1, and 32–64 scans/t_1. All spectra were referenced with external TSP-d4. Data processing and analysis were performed using Felix software (version 2001, Accelrys, San Diego, CA, USA) with shifted (60–90 degrees) square sinebell apodization and polynomial baseline correction for NOESY data.

Distance restraints and molecular modelling

Approximate interproton distance restraints were calculated using the isolated two-spin approximation relationship, $r_{ij} = r_{kl}(\sigma_{kl}/\sigma_{ij})^{1/6}$, where σ_{ij} and σ_{kl} are the NOE intensities for the atom pairs i, j and k, l separated by distances r_{ij} and r_{kl}, respectively. A total of 17 distance restraints were used for compound **19** and 4 for compound **10**. Restrained energy minimizations were performed with the software Insight II/Discover (Version 2005, Accelrys, San Diego, CA, USA), using the set of distance restraints determined by NMR. The selected force field was CVFF, and, to shorten the range of Coulomb interaction, a distance-dependent relative dielectric constant, ε_r, was used ($\varepsilon_r = 4r$). The structure was subjected to 2500 iterations of steepest descent minimization, followed by 2500 iterations of conjugate gradient minimization and the convergence of minimization was followed until the RMS derivative was less than 0.01 kcal mol^{-1}.

MALDI-TOF experiments

Mass spectra were acquired for all RAFT conjugates in a MALDI-TOF/TOF UltraFlex III mass spectrometer equipped with a nitrogen laser (Bruker-Daltonics, Bremen, Germany) using an external calibration of Protein Mixture 2 standard (Bruker-Daltonics, Germany). A 50 mg mL^{-1} solution of 2,5-dihydroxybenzoic acid (DHB) in 50% CH_3CN/0.1% CF_3COOH was used as the MALDI matrix and a 1.0 μL of pre-treated sample dissolved in water was, after drying, overlaid with 0.5 μL of the matrix solution on the target. The MALDI-TOF positive spectra were collected in linear mode. Every sample before mass spectrometric analysis was diluted in 20 μL 0.1% CF_3COOH and pre-treated in an OligoR3 (Applied Biosystems, CA, USA) reverse phase microcolumn. The prepared OligoR3 microcolumn (in Eppendorf gel-loader tips) was regenerated with 100 μL 80% CH_3CN, 0.1% CF_3COOH, washed with 100 μL 0.1% CF_3COOH, and after loading 20 μL of sample, washed again with 50 μL 0.1% CF_3COOH, 100 μL 100 mM CH_3COONH_4 (pH 8.1), and 50 μL 0.1% CF_3COOH. To elute a sample, 40 μL of 80% CH_3CN, 0.1% CF_3COOH was used, dried in a Speed-Vac, dissolved in 7 μL of deionized water and loaded onto the MALDI target.

Enzyme-linked lectin assay (ELLA)

96-well microtiter plates (Nunc, MaxiSorp, Vienna, Austria) were coated with polymeric α-D-mannose (PAA-αMan, 100 μL per well, diluted from a stock solution of 5 μg mL^{-1} in 0.01 M phosphate-buffered saline (PBS), pH 7.4, containing 0.1 mM Ca^{2+} and 0.1 mM Mn^{2+} for 1 h at 37 °C. The wells were then washed with PBS containing 0.05% (v/v) Tween 20 (T-PBS, 3 × 100 μL per well). The washing procedure was repeated after each incubation throughout the assay. The wells were then blocked with BSA in PBS (3% w/v, 100 μL per well) at 37 °C for 1 h. After washing, the wells were filled with 100 μL of serial dilutions of peroxidase-labelled concanavalin A (ConA-HRP) from 10^{-1}–10^{-7} mg mL^{-1} in 0.01 M PBS (pH 7.4) containing 0.1 mM Ca^{2+}, 0.1 mM Mn^{2+} and BSA (0.3% w/v) and incubated at 37 °C for 1 h. The plates were washed with T-PBS (3 × 100 μL per well) then the colour was developed using 100 μL per well of 0.05 M phosphate-citrate buffer containing *O*-phenylenediamine dihydrochloride (OPD, 0.4 mg mL^{-1}) and urea hydrogen peroxide (0.4 mg mL^{-1}). The reaction was stopped after 10 min by adding H_2SO_4 (30% v/v, 50 μL per well) and the absorbance was measured at 490 nm in each well. Blank wells contained citrate-phosphate buffer. The concentration of ConA-HRP conjugate that read absorbance between 0.8 and 1 was used for inhibition experiments.

Inhibition experiments

The microtiter plates were coated with PAA-αMan as described previously. Each inhibitor was added in serial two-fold dilutions (60 μL per well) in PBS with ConA-HRP (60 μL) at the desired concentration on Nunclon (Delta) microtiter plates and incubated for 1 h at 37 °C. The above solutions (100 μL) were then transferred to the mannose-polymer-coated microplates, which were incubated for 1 h at 37 °C. The plates were washed with T-PBS and the OPD substrate was added (100 μL per well). Colour development was stopped after 10 min and the absorbances were measured using a microtiter plate reader. The percentage inhibition was plotted against the logarithm of the concentration of the sugar derivatives. A sigmoidal curve was fitted and the concentration at 50% inhibition of binding of the ConA to

polymeric mannose-coated microtiter plate wells was determined (IC_{50}). The percentages of inhibition were calculated as given in eqn 1, where A = absorbance.

$$\% \text{ inhibition} = (A_{(\text{no inhibitor})} - A_{(\text{with inhibitor})})/A_{(\text{no inhibitor})} \times 100 \quad (1)$$

The IC_{50} values obtained from several independently performed tests were in the range of ±17%. Nevertheless, the relative inhibition values calculated from independent series of data were highly reproducible.

Acknowledgements

This work was supported by Université Joseph Fourier, Centre National de la Recherche Scientifique (CNRS) and EU ESF COST Chemistry project D34. We thank the NanoBio Program for access to the facilities of the Chemistry Platform. Further, this work was supported by grants LC06010 and MSM21620808 from the Ministry of Education of the Czech Republic, 305/09/H008 from the Czech Science Foundation, and by an Institutional Research Concept for the Institute of Microbiology (AVOZ50200510).

Notes and references

1 (*a*) H. J. Gabius, (Ed), *The Sugar Code. Fundamentals of Glycosciences*, Wiley-VCH, Weinheim, 2009; (*b*) M. Ambrosi, N. R. Cameron and B. G. Davis, *Org. Biomol. Chem.*, 2005, **3**, 1593–1608; (*c*) C. R. Bertozzi and L. L. Kiessling, *Science*, 2001, **291**, 2357–2354; (*d*) D. H. Dube and C. R. Bertozzi, *Nat. Rev. Drug Discovery*, 2005, **4**, 477–488.

2 (*a*) Y. C. Lee and R. T. Lee, *Acc. Chem. Res.*, 1995, **28**, 321–327; (*b*) M. Mammen, S. K. Choi and G. M. Whitesides, *Angew. Chem., Int. Ed.*, 1998, **37**, 2754–2794; (*c*) J. J. Lundquist and E. J. Toone, *Chem. Rev.*, 2002, **102**, 555–578; (*d*) T. K. Dam and C. F. Brewer, *Chem. Rev.*, 2002, **102**, 387–429.

3 (*a*) Y. M. Chabre and R. Roy, *Adv. Carbohydr. Chem. Biochem.*, 2010, **63**, 165–393; (*b*) A. Imberty, Y. M. Chabre and R. Roy, *Chem.–Eur. J.*, 2006, **14**, 7490–7499; (*c*) K. J. Doores, D. O. Gamblin and B. G. Davis, *Chem.–Eur. J.*, 2006, **12**, 656–665.

4 (*a*) P. I. Kitov, J. M. Sadowska, G. Mulvey, G. D. Armstrong, H. Ling, N. S. Pannu, R. J. Read and D. R. Bundle, *Nature*, 2000, **403**, 669–672; (*b*) M. Touaibia, A. Wellens, T. C. Shiao, Q. Wang, S. Sirois, J. Bouckaert and R. Roy, *ChemMedChem*, 2007, **2**, 1190–1201 c).

5 (*a*) J. E. Gestwicki, C. W. Cairo, L. E. Strong, K. A. Oetjen and L. L. Kiessling, *J. Am. Chem. Soc.*, 2002, **124**, 14922–14933; (*b*) L. L. Kiessling, J. E. Gestwicki and L. E. Strong, *Angew. Chem., Int. Ed.*, 2006, **45**, 2348–2368; (*c*) R. J. Pieters, *Org. Biomol. Chem.*, 2009, **7**, 2013–2025; (*d*) N. Rockendorf and T. K. Lindhorst, *Top. Curr. Chem.*, 2001, **217**, 201–238.

6 For recent reviews, see: (*a*) V. Ladmiral, E. Melia and D. M. Haddleton, *Eur. Polym. J.*, 2004, **40**, 431–449; (*b*) B. Voit and D. Appelhans, *Macromol. Chem. Phys.*, 2010, **211**, 727–735.

7 (*a*) K. Křenek, M. Kuldová, K. Hulíková, I. Stibor, P. Lhoták, M. Dudič, J. Budka, H. Pelantová, K. Bezouška, A. Fišerová and V. Křen, *Carbohydr. Res.*, 2007, **342**, 1781–1792; for recent reviews, see: (*b*) L. Baldini, A. Casnati, F. Sansone and R. Ungaro, *Chem. Soc. Rev.*, 2007, **36**, 254–266; (*c*) A. Dondoni and A. Marra, *Chem. Rev.*, 2010, **110**, 4949–4977.

8 For a recent review, see: D. A. Fulton and J. F. Stoddart, *Bioconjugate Chem.*, 2001, **12**, 655–672.

9 For recent reviews, see: (*a*) P. Niederhafner, J. Šebestík and J. Ježek, *J. Pept. Sci.*, 2008, **14**, 2–43; (*b*) P. Niederhafner, J. Šebestík and J. Ježek, *J. Pept. Sci.*, 2008, **14**, 44–65.

10 For recent reviews, see: (*a*) R. Roy, *Trends Glycosci. Glycotechnol.*, 2003, **15**, 291–310; (*b*) M. J. Cloninger, *Curr. Opin. Chem. Biol.*, 2002, **6**, 742–748.

11 O. Renaudet, *Mini-Rev. Org. Chem.*, 2008, **5**, 274–286.

12 For selected references, see: (*a*) K. Matsuura, M. Hibino, Y. Yamada and K. Kobayashi, *J. Am. Chem. Soc.*, 2001, **123**, 357–358; (*b*) C. Bouillon, A. Meyer, S. Vidal, A. Jochum, Y. Chevolot, J.-P. Cloarec, J.-P. Praly, J.-J. Vasseur and F. Morvan, *J. Org. Chem.*, 2006, **71**, 4700–4702; (*c*) K. Gorska, K.-T. Huang, O. Chaloin and N. Winssinger, *Angew. Chem., Int. Ed.*, 2009, **48**, 7695–7700.

13 J.-F. Nierengarten, J. Iehl, V. Oerthel, M. Holler, B. M. Illescas, A. Munoz, N. Martin, J. Rojo, M. Sanchez-Navarro, S. Cecioni, S. Vidal, K. Buffet, M. Durka and S. P. Vincent, *Chem. Commun.*, 2010, **46**, 3860–3862.

14 For selected reviews, see: (*a*) J. M. de la Fuente and S. Penadés, *Biochim. Biophys. Acta, Gen. Subj.*, 2006, **1760**, 636–651; (*b*) M. Marradi, M. Martín-Lomas and S. Penadés, *Adv. Carbohydr. Chem. Biochem.*, 2010, **64**, 211–290.

15 (*a*) D. Boturyn, E. Defrancq, G. T. Dolphin, J. Garcia, P. Labbé, O. Renaudet and P. Dumy, *J. Pept. Sci.*, 2008, **14**, 224–240; (*b*) O. Renaudet, J. Garcia, D. Boturyn, N. Spinelli, E. Defrancq, P. Labbé and P. Dumy, *Int. J. Nanotechnol.*, 2010, **7**, 738–752.

16 O. Renaudet and P. Dumy, *Org. Lett.*, 2003, **5**, 243–245.

17 V. Duléry, O. Renaudet, M. Wilczewski, A. Van der Heyden, P. Labbé and P. Dumy, *J. Comb. Chem.*, 2008, **10**, 368–371.

18 (*a*) O. Renaudet, G. Dasgupta, I. Bettahi, A. Shi, A. B. Nesburn, P. Dumy and L. BenMohamed, *PLoS One*, 2010, **5**, e11216; (*b*) O. Renaudet, K. Křenek, I. Bossu, P. Dumy, A. Kádek, D. Adámek, O. Vaněk, D. Kavan, R. Gažák, M. Šulc, K. Bezouška and V. Křen, *J. Am. Chem. Soc.*, 2010, **132**, 6800–6808; (*c*) O. Renaudet, L. BenMohamed, G. Dasgupta, I. Bettahi and P. Dumy, *ChemMedChem*, 2008, **3**, 737–741; (*d*) I. Bettahi, G. Dasgupta, O. Renaudet, A. A. Chentoufi, X. Zhang, D. Carpenter, S. Yoon, P. Dumy and L. BenMohamed, *Cancer Immunol. Immunother.*, 2009, **58**, 187–200; (*e*) S. Grigalevicius, S. Chierici, O. Renaudet, R. Lo-Man, E. Dériaud, C. Leclerc and P. Dumy, *Bioconjugate Chem.*, 2005, **5**, 1149–1159.

19 (*a*) N. Dendane, A. Hoang, O. Renaudet, F. Vinet, P. Dumy and E. Defrancq, *Lab Chip*, 2008, **8**, 2161–2163; (*b*) M.-P. Dubois, C. Gondran, O. Renaudet, P. Dumy, H. Driguez, S. Fort and S. Cosnier, *Chem. Commun.*, 2005, 4318–4320; (*c*) M. Wilczewski, A. Van der Heyden, O. Renaudet, P. Dumy, L. Coche-Guérente and P. Labbé, *Org. Biomol. Chem.*, 2008, **6**, 1114–1122.

20 W. B. Turnbull and J. F. Stoddart, *Rev. Mol. Biotechnol.*, 2002, **90**, 231–255.

21 (*a*) H. C. Hang and C. R. Bertozzi, *Acc. Chem. Res.*, 2001, **34**, 727–736; (*b*) K. Lu, Q.-P. Duan, L. Ma and D.-X. Zhao, *Bioconjugate Chem.*, 2010, **21**, 187–202.

22 (*a*) F. Peri and F. Nicotra, *Chem. Commun.*, 2004, 623–627; (*b*) J. M. Langenhan and J. S. Thorson, *Curr. Org. Synth.*, 2005, **2**, 59–81.

23 (*a*) F. Peri, P. Dumy and M. Mutter, *Tetrahedron*, 1998, **54**, 12269–12278; (*b*) J. M. Langenhan, N. R. Peters, I. A. Guzei, F. M. Hoffmann and J. S. Thorson, *Proc. Natl. Acad. Sci. U. S. A.*, 2005, **102**, 12305–12310; (*c*) A. V. Gudmundsdottir, C. E. Paul and M. Nitz, *Carbohydr. Res.*, 2009, **344**, 278–284.

24 S. Cao, F. D. Tropper and R. Roy, *Tetrahedron*, 1995, **51**, 6679–6686.

25 For selected references, see: (*a*) E. C. Rodriguez, L. A. Marcaurelle and C. R. Bertozzi, *J. Org. Chem.*, 1998, **63**, 7134–7135; (*b*) L. A. Marcaurelle, Y. Shin, S. Goon and C. R. Bertozzi, *Org. Lett.*, 2001, **3**, 3691–3694; (*c*) X. Chen, G. S. Lee, A. Zettl and C. R. Bertozzi, *Angew. Chem. Int. Ed.*, 2004, **43**, 6112–6116; (*d*) P. R. Andreana, W. Xie, H. N. Cheng, L. Qiao, D. J. Murphy, Q.-M. Gu and P. G. Wang, *Org. Lett.*, 2002, **4**, 1863–1866; (*e*) O. Renaudet and P. Dumy, *Tetrahedron*, 2002, **58**, 2127–2135; (*f*) O. Renaudet and P. Dumy, *Eur. J. Org. Chem.*, 2008, 5383–5386; (*g*) O. Renaudet and J.-L. Reymond, *Org. Lett.*, 2003, **5**, 4693–4696; (*h*) J. Tejler, H. Leffler and U. J. Nilsson, *Bioorg. Med. Chem. Lett.*, 2005, **15**, 2343–2345; (*i*) H. Brunner, M. Schönherr and M. Zabel, *Tetrahedron: Asymmetry*, 2003, **14**, 1115–1122; (*j*) D. Lagnoux, T. Darbre, M. Lienhard Schmitz and J.-L. Reymond, *Chem.–Eur. J.*, 2005, **11**, 3941–3950.

26 O. Renaudet and P. Dumy, *Tetrahedron Lett.*, 2001, **42**, 7575–7578.

27 O. Renaudet and P. Dumy, *Open Glycoscience*, 2008, **1**, 1–7.

28 O. Renaudet and P. Dumy, *Org. Biomol. Chem.*, 2006, **4**, 2628–2636.

29 O. Renaudet and P. Dumy, *Tetrahedron Lett.*, 2004, **45**, 65–68.

30 Y. Singh, O. Renaudet, E. Defrancq and P. Dumy, *Org. Lett.*, 2005, **7**, 1359–1362.

31 K. F. Geoghegan and J. G. Stroh, *Bioconjugate Chem.*, 1992, **3**, 138–146.

32 V. Duléry, O. Renaudet and P. Dumy, *Tetrahedron*, 2007, **63**, 11952–11958.

33 (*a*) J. Kalia and R. T. Raines, *Angew. Chem., Int. Ed.*, 2008, **47**, 7523–7526; (*b*) N. Spinelli, O. P. Edupuganti, E. Defrancq and P. Dumy, *Org. Lett.*, 2007, **9**, 219–222.

34 E. K. Woller and M. J. Cloninger, *Biomacromolecules*, 2001, **2**, 1052–1054.

35 K. Wüthrich, *NMR of Proteins and Nucleic Acids*, John Wiley and Sons, New York, (1986).
36 N. Nazarpack-Kandlousy, I. V. Chernushevich, L. J. Meng, Y. Yang and A. V. Eliseev, *J. Am. Chem. Soc.*, 2000, **122**, 3358–3366.
37 Y. Mechref and M. V. Novotny, *Chem. Rev.*, 2002, **102**, 321–369.
38 D. Pagé, D. Zanini and R. Roy, *Bioorg. Med. Chem.*, 1996, **4**, 1949–1961.
39 (*a*) T. Poethko, M. Schottelius, G. Thumshirn, M. Herz, R. Haubner, G. Henriksen, H. Kessler, M. Schwaiger and H.-J. Wester, *Radiochim. Acta*, 2004, **92**, 317–327; (*b*) E. H. Nardin, J. M. Calvo-Calle, G. A. Oliveira, P. Clavijo, R. Nussenzweig, R. Simon, W. Zeng and K. Rose, *Vaccine*, 1998, **16**, 590–600.
40 L. Braunschweiler and R. R. Ernst, *J. Magn. Reson.*, 1983, **53**, 521–528.
41 U. Piantini, O. W. Sørensen and R. R. Ernst, *J. Am. Chem. Soc.*, 1982, **104**, 6800–6801.
42 J. Jeener, B. H. Meier, P. Bachmann and R. R. Ernst, *J. Chem. Phys.*, 1979, **71**, 4546–4553.
43 T. L. Hwang and A. J. Shaka, *J. Magn. Reson., Ser. A*, 1995, **112**, 275–279.
44 A. J. Shaka, C. J. Lee and A. Pines, *J. Magn. Reson.*, 1988, **77**, 274–293.